

Effect of anionic concentration on the structural and optical properties of nanostructured ZnS thin films



T.A. Safeera ^a, N. Johns ^{b,c}, E.I. Anila ^{a,*}

^a Optoelectronic & Nanomaterial's Research Lab, Department of Physics, Union Christian College, Aluva 683102, Kerala, India

^b Department of Physics, St.Thomas College, Thrissur 680001, Kerala, India

^c Department of Metallurgical Engineering and Material Science, IIT, Mumbai 400076, India

ARTICLE INFO

Article history:

Received 19 February 2016

Received in revised form

19 March 2016

Accepted 27 March 2016

ABSTRACT

Nanostructured Zinc Sulfide (ZnS) thin films with wurtzite structure were prepared by chemical spray pyrolysis method at low temperature. The effect of sulfur concentration on the structural and optical properties of ZnS thin films was studied. The films were analysed by x-ray diffraction (XRD), scanning electron microscopy (SEM), energy dispersive X-ray spectroscopy (EDX), UV–Vis spectroscopy and photoluminescence (PL). Nano grain formation of ZnS was observed from XRD and SEM. Variation in band gap of different films is in agreement with size effects. But there is a red shift in the band gap of these films compared to bulk ZnS. This is due to band tailing effect experienced by the films due to the presence of large number of defects which was verified by PL spectrum. The overall emission was blue in colour for all the films and it was confirmed by Commission International d'Eclairage (CIE) diagram.

© 2016 Elsevier B.V. All rights reserved.

Keywords:

Chemical spray pyrolysis

Optical material

Photoluminescence

Chromaticity diagram

1. Introduction

Zinc sulfide (ZnS) is a well-known optoelectronic semiconductor material having wider range of applications in a variety of fields. The wide – direct bandgap of 3.5–3.8 eV [1,2], the smaller excitonic radius of 2.5 nm [3], polymorphism in crystal structure [4] etc. makes it as a prominent compound in the optoelectronic world. Their application includes light emitting diodes [5,6], infrared windows in solar cells [7,8], lasers [9], sensors [10], display devices [11,12], scintillation detectors [13] etc.

A variety of physical and chemical deposition methods like sputtering [14,15], chemical vapor deposition [16], sol gel [17], chemical bath deposition [18,19], chemical spray pyrolysis [20,21] etc are available for the synthesis of ZnS. In these methods chemical spray pyrolysis (CSP) method is the one which results in the large scale fabrication of uniform, well-crystalline and high quality thin films. It is a simple, low cost and environmental friendly technique among other fabrication methods.

The concentration of constituent elements plays an important role in the formation of the final compound. As the ratio between the elements varies, the properties of the mixture change and it is

more evident in the nano regime. In the case of ZnS, Sulfur (S) to Zinc (Zn) ratio is one of the key parameters which determine the properties of the final compound. Z. Q. Li et al. reported the effect of S/Zn ratio on the formation of ZnS films by chemical bath deposition technique in which they obtained good quality films for S/Zn ratio of six [22]. Formation of ZnS quantum dots having wurtzite crystal structure at a lower temperature of 350 °C by chemical spray pyrolysis method was reported earlier [20]. In the present work, we studied the variation in the structural and optical properties of the zinc sulfide (ZnS) thin films with sulfur (S) concentration. The change in S results in apparent changes in the ZnS thin film formation and their properties.

The fabricated thin films were analyzed structurally using x-ray diffraction (XRD) method. Scanning electron microscopy (SEM) was used for the surface morphological analysis and energy dispersive X-ray spectroscopy (EDX) was used for the elemental analysis of the prepared film. The optical properties were studied by techniques like UV–Vis absorption & transmission spectroscopy and photoluminescence (PL).

2. Experimental

The ZnS thin films were synthesized by chemical spray pyrolysis method. The spray solution was formed by drop wise mixing of thiourea [$\text{CH}_4\text{N}_2\text{S}$, Merck, 99%] with 1 M (1 M) solution of zinc

* Corresponding author.

E-mail address: anilaei@gmail.com (E.I. Anila).

chloride [ZnCl₂, Merck, 95%] in distilled water. The concentration of Zn is fixed at a value of 1 M and that of S is varied from 0.5 M to 2.5 M. The solution was sprayed at the rate of 20 ml/min, to a preheated glass substrate kept at a temperature of 350 °C. The detailed explanation for the theory of CSP and experimental setup is explained elsewhere [20].

Bruker AXS D8 advance X-ray diffractometer using Cu-K α lines ($\lambda = 1.5406\text{Å}$) was used for recording XRD pattern of the synthesized thin films. Using JEOL JSM 7600F field emission scanning electron microscope and JEOL JSM 6390LV scanning electron microscope, surface morphology and elemental composition of ZnS were studied. The optical analysis like absorbance and transmission of the films were done using Shimadzu UV–VIS–NIR spectrophotometer. Various emission centers in the prepared thin films were noted using PL measurements with Horiba Fluoromax-4C spectrofluorometer.

3. Results and discussion

The crystalline quality of the synthesized films and effect of S concentration on it were noted using the nondestructive XRD technique and is depicted in Fig. 1. In the sample synthesized with 0.5 M sulfur concentration ZnO phase is found to be dominant with S/Zn ratio 0.01 and it matches with JCPDS 79-0208. The reduced concentration of S in the precursor compared to zinc (1 M) may be the reason for the formation of ZnO. For all other cases, wurtzite structured ZnS films, matching with JCPDS file no: 75-1534 was formed. Good crystalline quality and sharp peaks are observed for the S concentration of 1 M. As the S molarity increases peaks becomes broader due to decrease in grain size. The smallest ZnS grain is for the concentration of 2.5 M.

Grain size (D) of the films were calculated using Debye – Scherrer's formula

$$D = \frac{0.9\lambda}{\beta \cos \theta} \quad (1)$$

where β is full width at half maximum, θ – glancing angle, λ – wavelength of light used. The lattice parameters of ZnS films were calculated from the relation,

$$d_{hkl} = \frac{1}{\sqrt{\frac{h^2+k^2}{a^2} + \frac{l^2}{c^2}}} \quad (2)$$

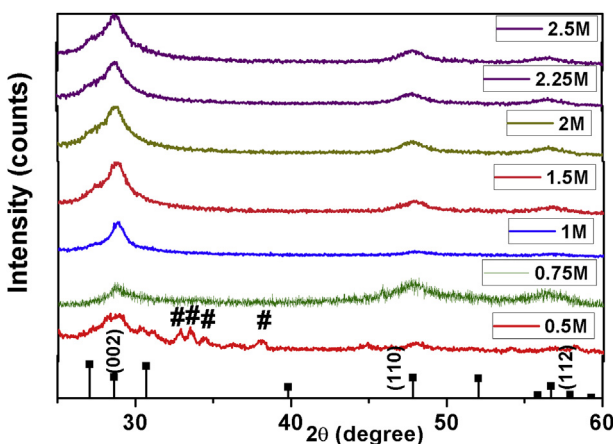


Fig. 1. X-ray diffractogram of ZnS thin films for various S concentrations [# - ZnO phase].

where d_{hkl} is the interplanar distance.

The lattice strain (ξ) produced and grain size (D) of ZnS thin films can be measured from the Williamson–Hall (WH) plot. The slope of the plot gives lattice strain and intercept leads to grain size value [23,24]. Fig. 2 shows the WH plot for various concentrations of S. For the sample with 1 M sulfur concentration, the strain in ZnS is positive and for all other samples negative strain is observed due to lattice compression. The relation employed is

$$\beta \cos \theta = \frac{0.9\lambda}{D} + 2\xi \sin \theta \quad (3)$$

The variation of lattice parameters, strain and grain size with S concentration is tabulated in Table 1.

As the S concentration increases, there is a peak shift to the lower 2θ values which leads to increase in interplanar distance and hence lattice parameters increase with S concentration [Table 1].

Variation in surface morphology of ZnS thin films with S concentration, in the micrometer range is illustrated in Fig. 3. For lowest S concentration, rod like structures can be seen [Inset of Fig. 3a], which may be ZnO rods formed due to lower sulfur to zinc ratio which is 0.01 according to EDX. Authors have reported the formation of ZnO nano nails using spray pyrolysis with the same precursors [25]. As S concentration increases rod like structures disappear and the pattern becomes broader and continuous. For 1 M sulfur concentration formation of ZnS quantum dots was reported earlier [20] [inset - Fig. 3b]. For all the samples, the grain size of ZnS film formed is around 5 nm as observed from XRD [Table 1]. The elemental composition obtained from EDX is shown in Fig. 4. From EDX, formation of ZnO phase for 0.5 M, S concentration was confirmed since S/Zn ratio is 0.01. The S/Zn ratios for other samples are tabulated in Table 2. There is a random change in S/Zn ratio in the films for different S concentrations compared to the ratio in spray solution, except for film with equal molarity (1 M). This may be due to the change in evaporation rate of S in the high temperature zone, for unequal sulphur and zinc concentrations in the spray solution.

The defects present in the fabricated films and their corresponding emissions were analyzed from the PL spectra. Fig. 5 represents emission spectra for an excitation wavelength of 320 nm. For the ZnO film, a broad emission centered at 392 nm and a less intense peak at 465 nm was observed. On comparison with band gap value of 3.5 eV, we can conclude that the former emission is related to the near band edge emission of ZnO [26,27]. The second peak is originated from the zinc vacancy (V_{Zn}) in the crystal lattice [25,28].

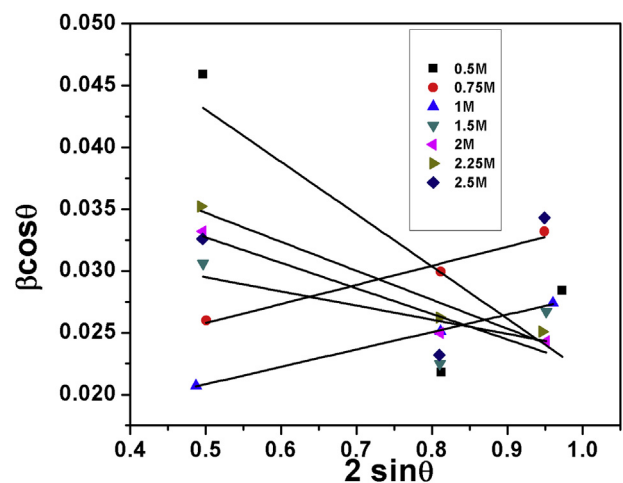
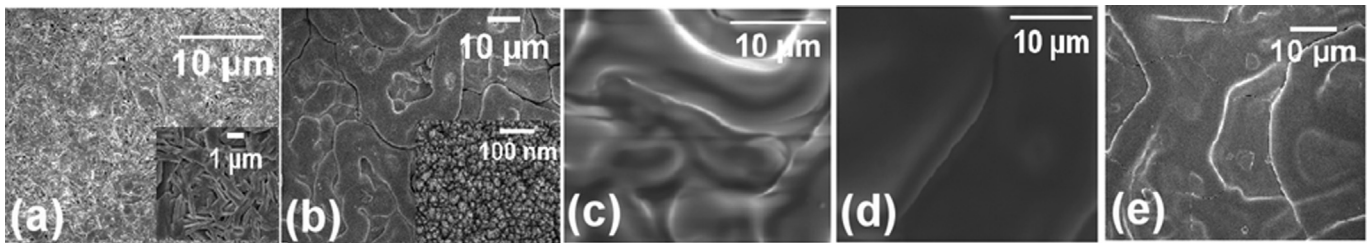
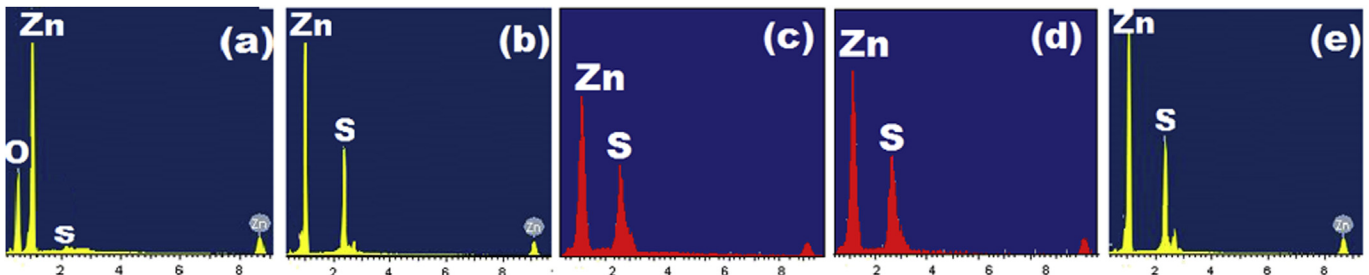


Fig. 2. Variation in W–H plot with S concentration.

Table 1

Effect of S concentration on lattice strain and grain size and band gap.

Sulfur concentration (M)	Lattice parameter (\AA)		Lattice strain	Crystallite size (nm)		Bandgap (eV)
	a = b	c		Scherrer's formula	WH plot	
0.5	2.68	6.22	-0.042	4.76	3.38	3.5
0.75	2.68	6.16	+0.015	5.81	5.23	3.35
1	2.69	6.17	+0.014	5.76	5.16	3.43
1.5	2.69	6.21	-0.011	5.30	4.94	3.45
2	2.69	6.21	-0.021	5.15	4.54	3.46
2.25	2.69	6.22	-0.02	4.87	4.48	3.47
2.5	2.69	6.22	-0.002	4.76	4.40	3.52

**Fig. 3.** SEM micrographs of ZnS (a) 0.5 M, (b) 1 M (c) 1.5 M, (d) 2 M and (e) 2.5 M of S concentration.**Fig. 4.** EDX spectra for the (a) 0.5 M, (b) 1 M (c) 1.5 M, (d) 2 M and (e) 2.5 M S concentration.**Table 2**

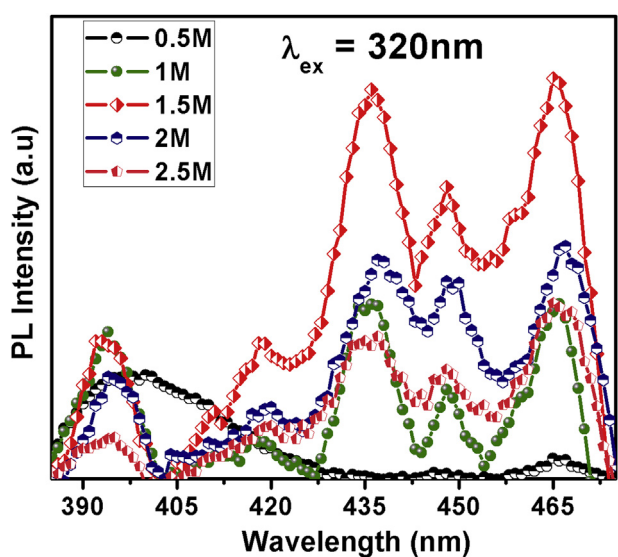
Variation of S/Zn ratio and CIE coordinates with S concentration.

Concentration (M)	S/Zn ratio	CIE coordinates	
		x	y
0.5	0.01	0.142	0.162
1	0.8	0.136	0.132
1.5	0.5	0.136	0.101
2	0.6	0.132	0.199
2.5	0.8	0.136	0.125

In the case of ZnS, PL spectra shows various defect level emissions arising from the native point defects like sulfur vacancy (V_S), zinc vacancy (V_{Zn}) and interstitial zinc (I_{Zn}). On varying the concentration, resulting emissions are from the same centers with wavelengths 394, 420, 436, 448 and 465 nm. The peak at 394 nm may be due to the transition between valence band and excitonic level. The interstitial zinc (I_{Zn}) present in the lattice is the origin of an emission at 420 nm [29,30]. The peak around 435 nm is due to the sulfur vacancy (V_S) [31–33]. The electron–hole recombination between the surface state and V_S leads to the emission around 447 nm [34,35]. The highly intense peak at 465 nm is attributed to the transition between the zinc and sulfur vacancy levels [36–38].

From EDX we can see that, S/Zn ratio in the ZnS thin film samples decreases or sulfur vacancy increases in the order 1, 2.5, 2 and 1.5 M concentrations of sulfur. Hence the integral intensity of sulfur

vacancy related emission should be maximum for the sample synthesized with 1.5 M sulfur concentration and it is clearly observed in the PL spectra [Fig. 5]. The variation in integral intensity

**Fig. 5.** Change in PL intensity with S concentration.

of all the samples for sulfur vacancy related emission is in agreement with S/Zn ratio. The intensity of I_{Zn} related emission is also in the same order.

On comparing the PL emission for samples with least (1 M) and maximum (2.5 M) sulfur concentrations, (sample with 0.5 M sulfur concentration is containing ZnO phase also) there is a blue shift in the peak values of the near band edge emission and sulfur vacancy related emission for 2.5 M sample compared to 1 M in accordance with the band gap variation. For the other two samples the change is random for different peaks which may be due to the overlapping of different vacancy related emissions and hence the lack of symmetry in the peaks.

Fig. 6 depicts the various energy bands present in the band gap due to the impurities in the lattice. The various emissions in the PL spectra are also represented in the band diagram. All the observed emissions lie in the blue region which is confirmed by the Commission International d'Eclairage (CIE) diagram [Fig. 7] with the CIE coordinates given in **Table 2**.

Here for all the films with ZnS phase the absorbance is uniform over a wide range on moving from near infrared region to UV and shows a sharp increase below 400 nm [Fig. 8] whereas the oxygen rich film shows a linear increase throughout the range with an absorption edge at 355 nm.

From the spectra, band gap values can be estimated using Tauc plot. Bardeen et al. [39] derived a relation

$$\alpha h\nu = A(h\nu - E_g)^\gamma \quad (4)$$

which is used for the band gap determination where α is absorption coefficient and $h\nu$ is incident photon energy. Extrapolation of linear portion of Tauc plot to energy axis will result in the band gap value [Fig. 9]. As S concentration in the precursor increases band gap value increases except for 0.5 M film with ZnO phase also. **Table 1** provides the band gap values with concentration of ZnS thin films. Even though there is a quantum confinement in the synthesized films, no band gap enhancement from bulk ZnS is observed. This is due to the band tailing effect resulting from the increased defect levels [40,41] verified from PL spectra.

There exists an inverse relationship between the grain size and band gap values in the nano regime [42]. The same is confirmed from **Fig. 10**, which represents variation of these with S concentration.

The synthesized films except 0.5 M film show low transmittance and it almost decreases with concentration in the visible range. The transmittance spectra showing these are depicted in **Fig. 11**.

4. Conclusions

Zinc sulfide thin films having wurtzite structure were prepared

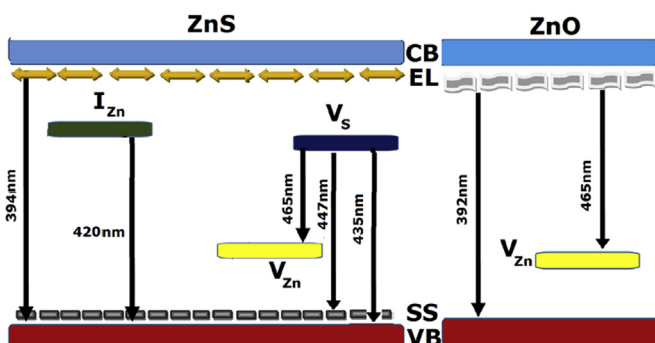


Fig. 6. Energy band diagram for ZnO/ZnS thin films.

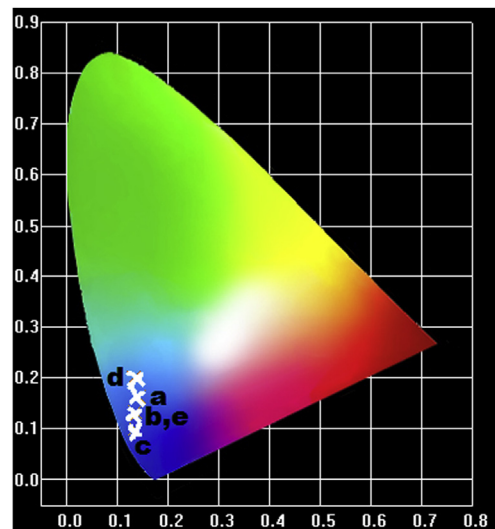


Fig. 7. CIE chromaticity diagram for Zn:S quantum dots[a-0.5 M, b-1 M, c-1.5 M, d-2 M, e-2.5 M].

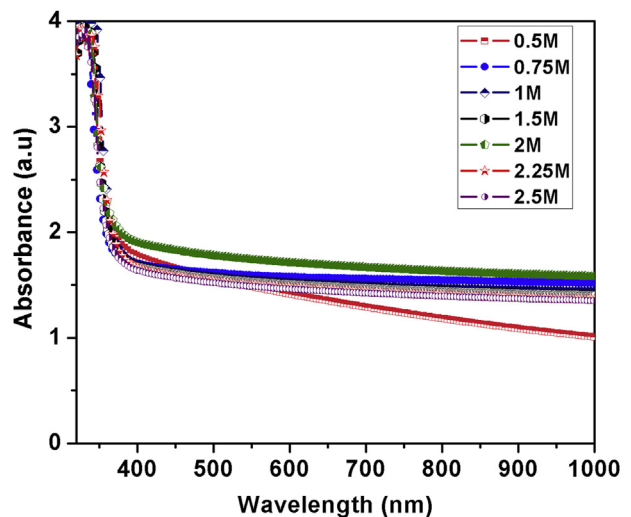


Fig. 8. Absorbance spectra of ZnS with S concentration.

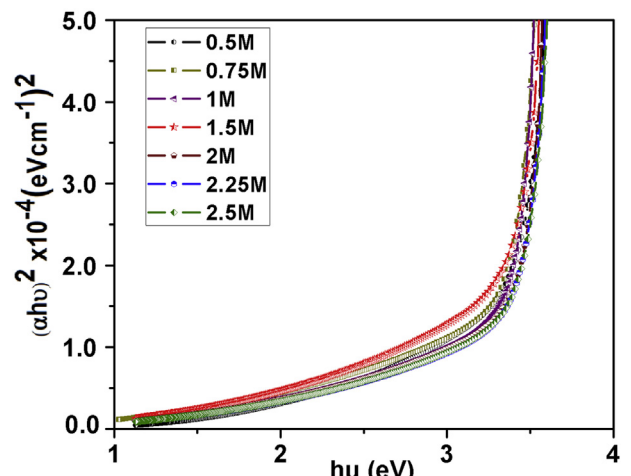


Fig. 9. Bandgap diagram for ZnS Quantum dots with S concentration.

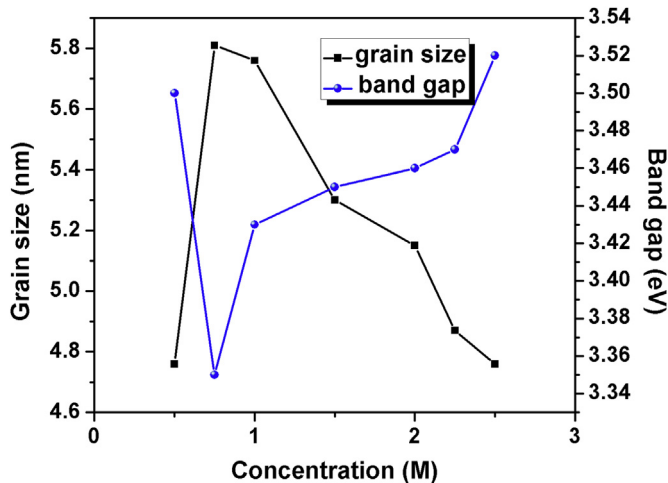


Fig. 10. Variation of grain size and bandgap with S concentration.

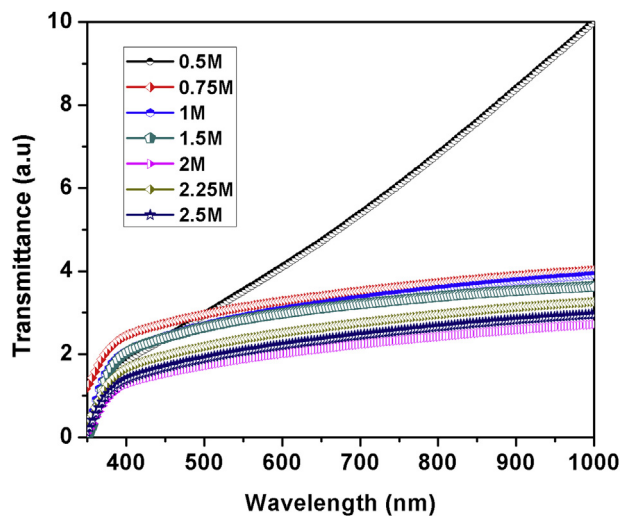


Fig. 11. Transmission spectra of ZnS thin films.

by chemical spray pyrolysis method at low temperature. The variation in structural, morphological and optical properties with S concentration was studied. Equal molar Zn: S resulted in good quality film. The grain size of all the samples are around 5 nm. Band gap of all ZnS films are less than bulk due to band tailing effect resulted from large number of defects as confirmed from PL spectra. The PL spectra gave blue emission for all films and they are in agreement with CIE diagram.

Acknowledgements

This work was financially supported by Science and Engineering Research Board (SERB), Department of Science and Technology, Government of India.

References

- [1] M.C. Lopez, J.P. Espinos, F. Martin, D. Leinen, J.R. Ramos Barrado, Growth of ZnS thin films obtained by chemical spray pyrolysis: the influence of precursors, *J. Cryst. Growth* 285 (2005) 66–75.
- [2] N. Fathy, R. Kobayashi, M. Ichimura, Preparation of ZnS thin films by the pulsed electrochemical deposition, *J. Mater. Sci. Eng. B* 107 (3) (2004) 271–276.
- [3] Mahdi Hasan Suhail, Structural and optical properties of ZnS, PbS, $Zn_{1-x}Pb_xS$, $Zn_xPb_{1-x}S$, $PbZn_xS_{1-x}$ thin films, *Indian J. Pure Appl. Phys.* 50 (2012) 380–386.
- [4] Li Ho, Faming Gao, Phase and morphology controlled synthesis of high quality ZnS nanocrystals, *J. Mater. Lett.* 65 (2011) 500–503.
- [5] Shiv P. Patel, J.C. Pivin, V.V. Siva Kumar, A. Tripathi, D. Kanjilal, Grain growth and structural transformation in ZnS nanocrystalline thin films, *Vacuum* 85 (2010) 307–311.
- [6] N. Katayama, S. Oda, H. Kukimoto, ZnS blue-light emitting diodes with an external quantum efficiency of times, *J. Appl. Phys. Lett.* 27 (1975) 697–699.
- [7] S. Velumani, J.A. Ascencio, Formation of ZnS nanorods by simple evaporation technique, *J. Appl. Phys. A* 79 (2004) 153–156.
- [8] Y.P. Venkata Subbaiah, P. Prathap, K.T. Ramakrishna Reddy, Structural electrical and optical properties of ZnS films deposited by close-spaced evaporation, *J. Appl. Surf. Sci.* 253 (2006) 2409–2415.
- [9] J.T. Hu, L.S. Li, W.D. Yang, L. Manna, L.W. Wang, A.P. Alivisatos, Linearly polarized emission from colloidal semiconductor quantum rods, *Science* 292 (2001) 2060–2063.
- [10] C.J. Murphy, Photophysical probes of DNA sequence directed structure and dynamics, *Adv. Photochem.* 26 (2001) 145–217.
- [11] Sakshi Sahare, S.J. Dhoble, Pranav Singh, Meera Ramrakhiani, Fabrication of ZnS: Cu/PVA nanocomposite electroluminescence devices for flat panel displays, *J. Adv. Mat. Lett.* 4 (2) (2013) 169–173.
- [12] Zhi-Gang Chen, Lina Cheng, Hong-Yi Xu, Ji-Zi Liu, Jin Zou, Takashi Sekiguchi, Gao Qing (Max) Lu, Hui-Ming Cheng, ZnS branched architectures as optoelectronic devices and field emitters, *J. Adv. Mater.* 22 (2010) 2376–2380.
- [13] S.A. McElhaney, J.A. Ramsey, M.L. Bauer, M.M. Chiles, A ruggedized ZnS(Ag)/epoxy alpha scintillation detector, *Nucl. Instrum. Methods Phys. Res. Sect. A Accel. Spectrom. Detect. Assoc. Equip.* 299 (1990) 111–114.
- [14] A. Nitta, K. Tanaka, Y. Maekawa, M. Kusabiraki, M. Aozasa, Effects of gas impurities in the sputtering environment on the stoichiometry and crystallinity of ZnS: Mn electroluminescent device active layers, *Thin Solid Films* 384 (2001) 261–268.
- [15] Q. He, H-bin Guo, J-jun Wei, S.J. Askari, H-bin Wang, S-yu Zhang, et al., Effect of HfO₂ thin films on ZnS substrates, *Thin Solid Films* 516 (2008) 4695–4699.
- [16] John S. McCloy, Barrett G. Potter, Photoluminescence in chemical vapor deposited ZnS: insight into electronic defects, *J. Opt. Mater. Express* 3 (2013) 1273–1278.
- [17] Y. Ian, Y. Bu, Sol-gel synthesis of ZnS (O, OH) thin films: Influence of precursor and process temperature on its optoelectronic properties, *J. Luminescence* 134 (2013) 423–428.
- [18] P. Roy, R. Ota Jyoti, S.K. Srivastava, Crystalline ZnS thin films by chemical bath deposition method and its characterization, *Thin Solid Films* 515 (2006) 1912–1917.
- [19] K.R. Bindu, P.V. Sreenivasan, Arturo I. Martinez, E.I. Anila, α -Axis oriented ZnS thin film synthesized by dip coating method, *J. Solgel Sci. Technol.* 68 (2013) 351–355.
- [20] T.A. Safeera, N. Johns, E.I. Anila, Arturo I. Martinez, P.V. Sreenivasan, R. Reshma, Mallick Sudhanshu, M.K. Jayaraj, Low temperature fabrication and characterization of wurtzite structured ZnS quantum dots by chemical spray pyrolysis, *J. Anal. Appl. Pyrolysis* 115 (2015) 96–102.
- [21] Tatjana Dedova, CSP Deposition of ZnS Thin Films and ZnO Nano Structured Layers (Thesis on Natural and exact science B69), Tallinn University of Technology Tallinn, Estonia, 2007.
- [22] Z.Q. Li, J.H. Shi, Q.Q. Liu, Z.A. Wang, Z. Sun, S.M. Huang, Effect of Zn/S ratios on the properties of chemical bath deposited zinc sulfide thin films, *Appl. Surf. Sci.* 257 (2010) 122–126.
- [23] W.H. Hall, G.K. Williamson, The diffraction pattern of Cold worked metals: I the nature of Extinction, in: Proceedings of the Physical Society (Section B-64), West Midlands, United Kingdom, 1951, pp. 937–946.
- [24] G.K. Williamson, W.H. Hall, X-ray Line Broadening from filed aluminium and wolfram, *Acta Metall.* 1 (1953) 22–31.
- [25] T.A. Safeera, N. Johns, P.V. Athma, P.V. Sreenivasan, E.I. Anila, Synthesis and Characterization of ZnO nanonails, *AIP Conf. Proc.* 1620 (2014) 572–577.
- [26] P.V. Athma, N. Johns, E.I. Anila, T.A. Safeera, Structural and optical characterization of potassium doped zinc oxide nanosheets, *Opt. Mater.* 38 (2014) 223–227.
- [27] E.M. Wong, P.C. Searon, ZnO quantum particle thin films fabricated by electro-phoretic deposition, *Appl. Phys. Lett.* 74 (1999) 2939–2941.
- [28] Nargis Bano, I. Hussain, Omer Nour, Magnus Willander, P. Klason, Anne Henry, *Semicond. Sci. Technol.* 24 (12) (2009) 125015.
- [29] J. Manam, V. Chatterjee, S. Das, A. Choubey, S.K. Sharma, Preparation characterization and study of optical properties of ZnS nanophosphor, *J. Luminescence* 130 (2010) 292–297.
- [30] D. Denzler, M. Olschewski, K. Sattler, Luminescence studies of localized gap states in colloidal ZnS nanocrystals, *J. Appl. Phys.* 84 (5) (1998) 2841–2845.
- [31] Aaron C. Small, James H. Johnston, Novel hybrid materials of cellulose fibres and doped ZnS nanocrystals, *J. Current Appl. Phys.* 8 (2008) 512–515.
- [32] Jian Cao, Jinghai Yang, Yongjun Zhang, Lili Yang, Yixin Wang, Maobin Wei, Yang Liu, Ming Gao, Xiaoyan Liu, Zhi Xie, Optimized doping concentration of manganese in zinc sulfide nanoparticles for yellow-orange light emission, *J. Alloys Compd.* 486 (2009) 890–894.
- [33] M.V. Limaye, S. Gokhale, S.A. Acharya, S.K. Kulkarni, Template-free ZnS nanorod synthesis by microwave irradiation, *Nanotechnology* 19 (2008) 415602.
- [34] Q. Wu, H. Cao, S. Zhang, X. Zhang, D. Rabinovich, Generation and optical

- properties of monodisperse wurtzite type ZnS microspheres, *Inorg. Chem.* 45 (18) (2006) 7316–7322.
- [35] R.N. Bhargava, Doped nanocrystalline materials – Physics and applications, *J. Lumin.* 70 (1996) 85–94.
- [36] K. Manzoor, S.R. Vadera, N. Kumar, T.R.N. Kutty, Synthesis and photoluminescent properties of ZnS nanocrystals doped with copper and halogen, *J. Mater. Chem. Phys.* 82 (2003) 718–725.
- [37] G.H. Blount, A.C. Sanderson, R.H. Bube, Effects of Annealing on the Photo-electronic Properties of ZnS Crystals, *J. Appl. Phys.* 38 (1967) 4409–4416.
- [38] A.E. Thomas, G.J. Russell, J. Woods, Self activated emission in ZnS and ZnSe, *J. Phys. C* 17 (1984) 6219–6228.
- [39] J. Bardeen, F.J. Blatt, L.H. Hall, R. Breekwuridge, B. Russel, T. Hahn, in: *Proceedings of Photoconductivity Conference in Atlantic City*, John Wiley, New York, 1956, p. 146.
- [40] J.I. Pankove, *Optical Process in Semiconductors*, Butterworth, London, UK, 1971.
- [41] Piet Van Mieghem, Theory of band tails in heavily doped semiconductors, *Rev. Mod. Phys.* 64 (3) (1992) 755–793.
- [42] T. Pradeep, *NANO: The essentials*, Tata McGraw-Hill Publishing Company Limited, New Delhi, Chapter 7, 196page.